Nanotechnology

Electrical Contacting of Glucose Oxidase in a Redox-Active Rotaxane Configuration**

*Eugenii Katz, Laila Sheeney-Haj-Ichia, and Itamar Willner**

Dedicated to Professor Mordecai Rabinovitz on the occasion of his 70th birthday

The electrical contacting of redox enzymes such as glucose oxidase, with electrodes is of fundamental importance for the development of amperometric biosensors[1] and biofuel cells.[2] The tethering of redox-active units to the enzyme[3] or the immobilization of the biocatalysts in redox-active polymers[4] have been reported as means of establishing electrical communication between the redox centers of enzymes and electrodes.

Recently, our laboratory reported the surface reconstitution of apo-proteins (e.g. apo-glucose oxidase (apo-GOx)) on cofactor-functionalized monolayers associated with electrodes as a general method to establish electrical communication between redox sites in proteins and electrodes. The reconstitution of apo-GOx on a relay-functionalized flavin adenine dinucleotide (FAD) monolayer (e.g. pyrroloquinoline quinone (PQQ) linked to FAD),[5] or on FAD-functionalized Au nanoparticles,[6] or on FAD-functionalized carbon nanotubes[7] proved to be effective means of bringing the redox enzyme into electrical contact with the electrodes, and unprecedented high electron-transfer turnover rates were observed.

One of the challenges is the electrochemical activation of the biocatalyzed oxidation or reduction of a substrate at the

[*] Dr. E. Katz, L. Sheeney-Haj-Ichia, Prof. I. Willner
Institute of Chemistry, The Hebrew University of Jerusalem
Jerusalem 91904 (Israel)
Fax: (+972) 2-652-7715
E-mail: willnea@vms.huji.ac.il

[**] This research (No. 101/00) is supported by the Israel Science Foundation.

  DOI: 10.1002/ange.200353455

lowest possible positive or negative potential, respectively, close to the thermodynamic potential of the respective enzyme. This feature is significant for biosensor devices in order to eliminate nonspecific redox processes under applied overpotentials, and of key importance in developing biocatalytic electrodes for biofuel-cell elements to extract maximum electrical power.

Rotaxanes are interesting supramolecular structures[8] and redox-active rotaxanes on surfaces have been used to assemble molecular electronic[9] and optoelectronic[10] devices. Herein we report the first glucose oxidase (GOx)-reconstituted FAD-stoppered redox-active rotaxane on a Au electrode. The reconstituted GOx is brought into electrical contact with the electrode by the redox-active rotaxane which operates as an electron-transfer mediator to allow the effective bioelectrocatalytic oxidation of glucose at −0.4 V versus SCE (saturated calomel electrode)—a value that is very close to the thermodynamic redox potential of the FAD cofactor ($E° = -0.51$ V versus SCE at pH 8.0).[11]

Scheme 1 outlines the assembly of the rotaxane system on a gold electrode. Cystamine was self-assembled as a monolayer on a Au electrode (step a). The functionalized electrode was then treated with glutaric dialdehyde (step b) and the resulting monolayer was treated with 1,4-diaminobenzene (**1**; step c) to yield the iminophenylamino-functionalized monolayer. The monolayer was further treated with glutaric dialdehyde (step d) and then with the electron acceptor cyclobis(paraquat-*p*-phenylene) (**2**; step e) to yield the supramolecular donor–acceptor complex with the diiminobenzene electron-donating unit. The resulting supramolecular structure was then stoppered with N^6-(2-aminoethyl)-FAD (**3**; step f) to generate the rotaxane structure consisting of **2** threaded onto the stoppered wire. Subsequently, apo-GOx was reconstituted on the FAD cofactor to generate the electrically contacted enzyme assembly (Scheme 2).

Stepwise modification of the electrode thus yields amino-functionalized surfaces after self-assembly of cystamine (step a) and after the covalent attachment of 1,4-diaminobenzene (step c), whereas the reactions with glutaric dialdehyde (steps b and d) result in the surface amino groups being blocked. The stepwise appearance and disappearance of the surface amino groups and the surface coverage of these groups were probed by electrochemical assay of the PQQ redox units immobilized on the amino functionalities.[12] The cyclic voltammograms of the PQQ-treated electrodes (not shown) demonstrate similar loading of the PQQ units (ca. 1×10^{-10} mol cm^{-2}) on the two amino-terminated monolayer structures generated upon the stepwise assembly of the system. The low limit of the concentration of the amino groups on the surface (ca. 1×10^{-10} mol cm^{-2}) generated after modification steps a and c, could be derived from the cyclic voltammograms of PQQ. On the other hand, attempts to induce a reaction between PQQ and the surfaces whose amino groups are blocked by glutaric dialdehyde did not yield any redox response of PQQ. These experiments confirmed the quantitative formation of the surface structures outlined in Scheme 1.

The amounts of surface-bound molecular components after each step of the electrode modification (ca. 1×10^{-10} mol cm^{-2}) were also calculated from quartz crystal microbalance (QCM) measurements performed upon the assembly of the monolayer on a Au–quartz piezoelectric crystal following a similar synthetic strategy. Formation of the supramolecular donor–acceptor complex between the redox-active rotaxane **2** and the diiminobenzene electron-donating units on the electrode surface was probed at various bulk concentrations of **2** by a chronocoulometric technique by means of Equation (1):[13]

$$Q = 2nFAD^{1/2}c\pi^{-1/2}t^{1/2} + Q_{dl} + nFA\Gamma_2 \quad (1)$$

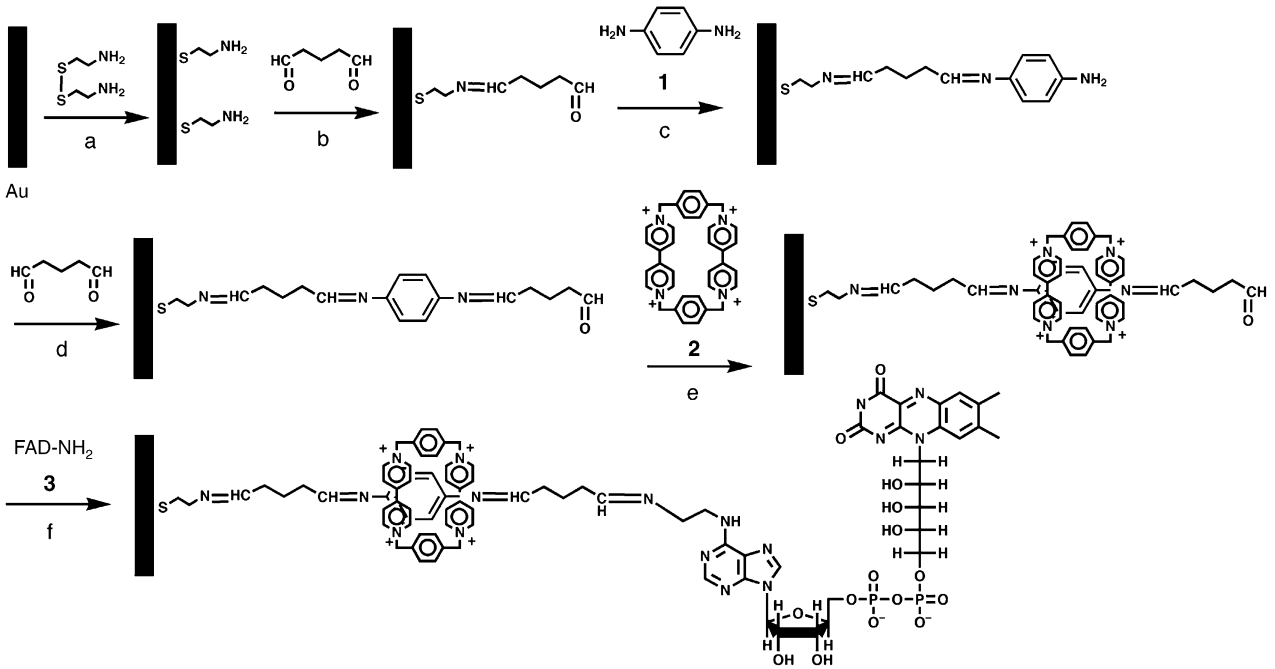

Scheme 1. Assembly of interlocked rotaxane redox units on a molecular string.

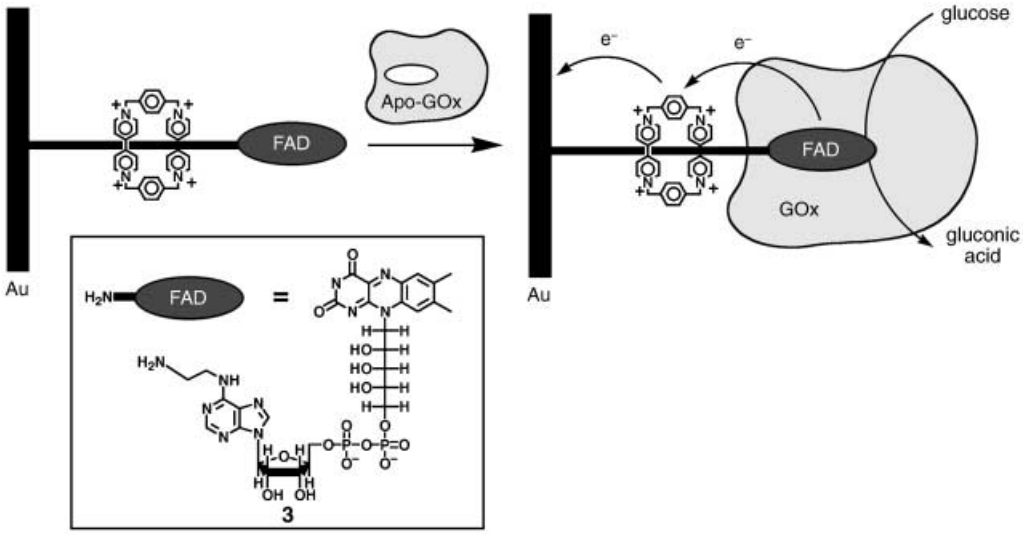

Scheme 2. The reconstitution of apo-GOx on the FAD–redox rotaxane molecular wire and the mechanism of the bioelectrocatalytic oxidation of glucose.

in which n is the number of electrons per molecule of **2** ($n=2$), F is the Faraday constant ($C\,equiv^{-1}$), A is the electrode area (cm^2), D is the diffusion coefficient ($cm^2\,s^{-1}$), c is the bulk concentration of **2** ($mol\,cm^{-3}$), Q_{dl} is the capacitance charge (C), and $nFA\Gamma_2$ is the charge associated with the reduction of the redox-active rotaxane **2** bound to the electron-donating sites on the surface; Γ_2 corresponds to the surface coverage of **2** ($mol\,cm^{-2}$).

Figure 1 A shows the chronocoulometric transients of the diiminobenzene-functionalized Au electrode in the absence of **2** (curve a) and in the presence of **2** at different bulk concentrations (curves b–d). The capacitance charge, Q_{dl}, was derived from the chronocoulometric transient measurement in the absence of the redox-rotaxane **2** by the extrapolation of its linear part to $t=0$. The sum of Q_{dl} and $nFA\Gamma_2$ was derived from the chronocoulometric transients for each bulk concentration of **2** by the extrapolation of their linear parts to $t=0$. As Q_{dl} and the surface coverages were known, the equilibrium Γ_2 values of the surface-bound **2** at variable bulk concentrations were calculated[13] (Figure 1 B). From this curve we were able to derive the association constant for the interaction between the acceptor **2** and the diimine donor sites to be approximately $K_a = 1\times10^4\,M^{-1}$. We then selected a bulk concentration of 0.3 mM for **2** to stopper the rotaxane with **3**. Under these conditions, about 80% of the diiminobenzene electron-donating units are associated with **2** in the rotaxane structure through the donor–acceptor complex. The surface coverage of **2** on the molecular wire is estimated to be approximately $0.8\times10^{-10}\,mol\,cm^{-2}$ and that of the cofactor-stopper approximately $1\times10^{-10}\,mol\,cm^{-2}$.

Microgravimetric quartz crystal microbalance (QCM) measurements provide a further means for following the association of **2** with the diiminobenzene-functionalized surface. The formation of the electron donor–acceptor complex of rotaxane **2** with the diiminobenzene moieties on the QCM surface is anticipated to cause a mass change (Δm) that

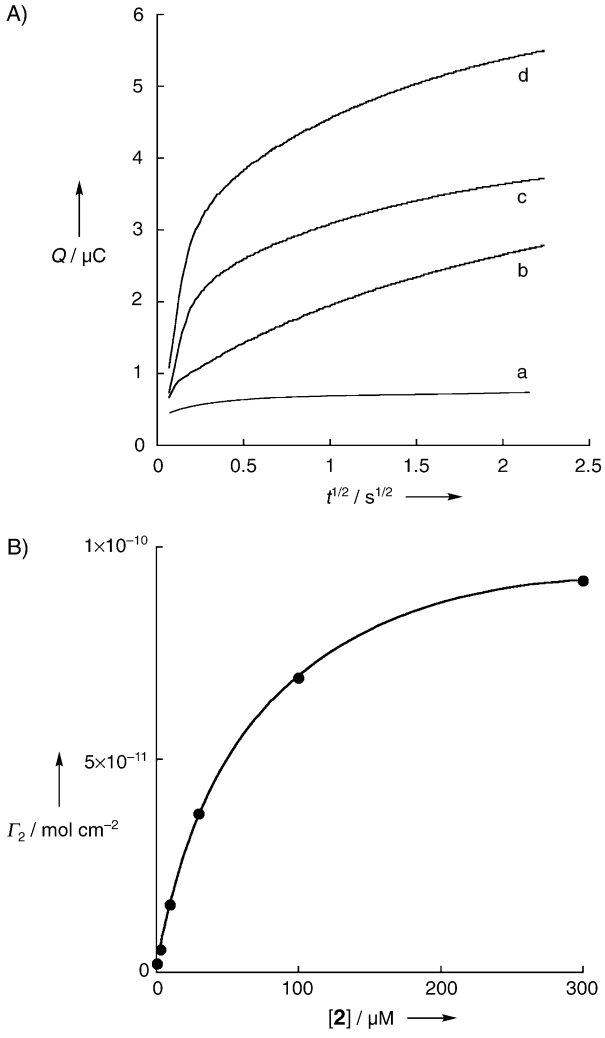

Figure 1. A) Chronocoulometric traces measured on the diiminobenzene-functionalized Au electrode upon application of a potential step from −0.35 to −0.50 V in the presence of **2** at various concentrations in the bulk solution in phosphate buffer (0.1 M, pH 8.0) under Ar: a) 0 μM, b) 10 μM, c) 30 μM, d) 100 μM. B) Variation of surface concentration of **2** (Γ_2) upon variation of its bulk concentration [**2**].

results in a frequency change (Δf) of the crystal according to the Sauerbrey equation [Eq. (2)]. (f_0 is the base frequency of

$$\Delta f = -2 f_0 \Delta m / A(\rho_q \mu_q)^{1/2} \quad (2)$$

the crystal, ρ_q is the quartz density (2.648 g cm^{-3}), μ_q is the shear modulus of the crystal (2.947×10^{11} dyn cm^{-2} for AT-cut quartz), and A is the surface area).[14]

A gold surface associated with the quartz crystal was modified with the diiminobenzene monolayer by the same procedure that was used for modification of the regular Au electrode. Figure 2A shows the time-dependent frequency change of the modified quartz crystal upon stepwise increase of the concentration of **2** in the solution. Interaction of the monolayer-modified quartz crystal with **2** results in a frequency decrease which implies a mass increase on the crystal. A time-dependent decrease of the crystal frequency is observed, and the frequency stabilizes to a constant Δf value which represents the equilibrium binding of **2** to the surface. As the bulk concentration of **2** increases, the Δf values increase; Figure 2B shows the steady-state values of Δf at various bulk concentrations of **2**. The Δf values were translated to the Δm values by using Equation (2), and then the respective surface-coverage values Γ_2 were derived (e.g. Γ_2 values of 3.8×10^{-11}, 6.9×10^{-11} and 9.2×10^{-11} mol cm^{-2} were obtained when the bulk concentrations of **2** were 30, 100 and 300 μM, respectively). The Γ_2 values derived from the microgravimetric measurements are similar to those obtained by the chronocoulometric technique. Thus, the association constant $K_a = 1 \times 10^4$ M^{-1} was confirmed by the QCM measurements. Importantly, the addition of **2** to a bare or cysteamine-modified quartz crystal did not result in any frequency changes of the quartz crystal, implying that no nonspecific adsorption occurred on the surface in the absence of the diiminobenzene electron-donating sites.

The formation of the supramolecular complex between the diiminobenzene π-donor moiety and the cyclobis(paraquat-*p*-phenylene) (**2**) π acceptor (Scheme 3) was further supported by UV/Vis absorbance and ^{1}H NMR spectroscopy experiments in solution. The addition of *p*-dipropyliminobenzene (**4**), as a model compound for the diiminobenzene unit in the monolayer structure, to a solution of **2** in acetone gave rise to a charge-transfer band at $\lambda_{max} = 608$ nm ($\varepsilon = 270$ M^{-1} cm^{-1}), Figure 3. We monitored the changes in the charge-transfer band upon variation of the concentration of **4** with respect to **2**, which allowed us to determine the association constant for the formation of the supramolecular complex between the two species. The association constant $K_a = 1.23 \times 10^4$ M^{-1} was derived from computer fitting of the

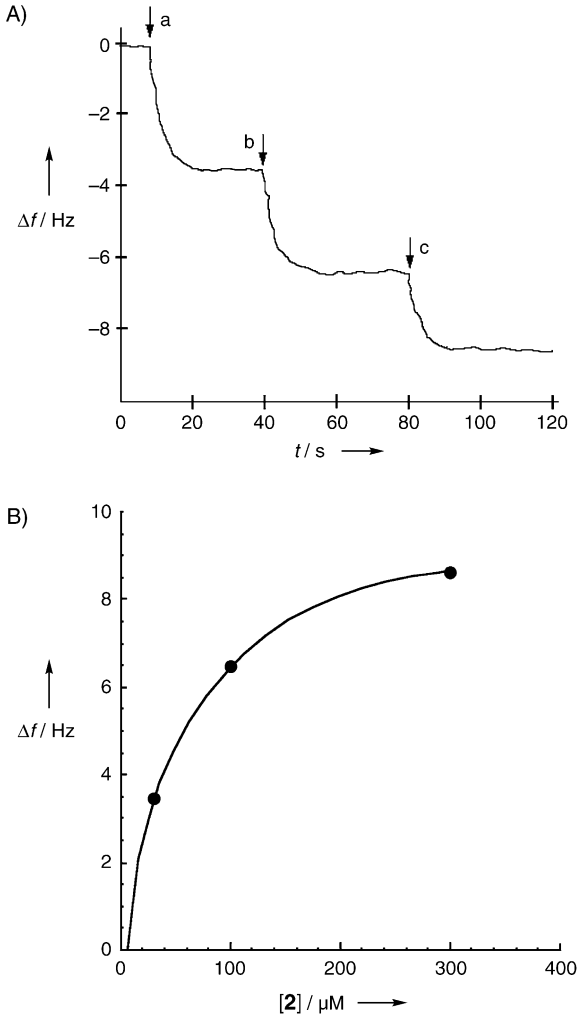

Figure 2. A) Time-dependent frequency changes of the diiminobenzene-functionalized Au/quartz crystal in the presence of **2** at different bulk concentrations in phosphate buffer (0.1 M, pH 8.0): a) 30 μM, b) 100 μM, c) 300 μM. B) Variation of the QCM frequency (Δf)with varying bulk concentrations of **2**.

experimental absorbance values (Figure 3, inset) to the absorbance expressed by Equation (3):[15]

$$A = l\varepsilon K_a [\mathbf{2}] [\mathbf{4}]/(1 + K [\mathbf{4}]) \quad (3)$$

(A is the absorbance of the charge-transfer complex measured at $\lambda_{max} = 608$ nm, l is the optical path length ($l = 1$ cm), ε is the molar absorptivity of the charge-transfer complex, K_a is the equilibrium constant for the formation of the complex,

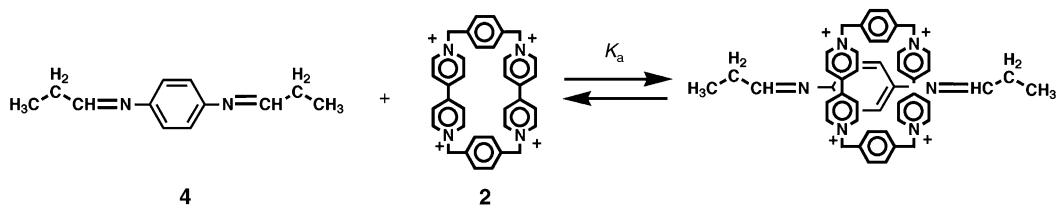

4 **2**

Scheme 3. Threading of the cyclophane **2** onto the model diimine compound **4** wire in solution.

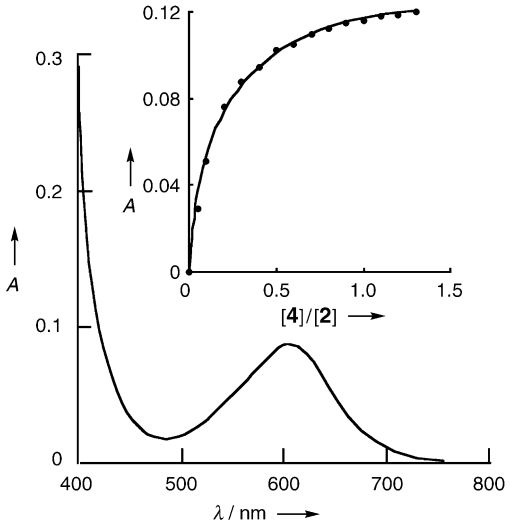

Figure 3. Absorption spectrum of cyclophane **2** (0.5 mM in acetone) in the presence of *p*-dipropyliminobenzene (**4**) (0.15 mM in acetone). Inset: Variation of the absorbance of the charge-transfer complex at $\lambda_{max} = 608$ nm, as a function of the molar ratio of **4** to **2**. The solid line represents computer fitting of the experimental points to Equation (3) using $K_a = 1.23 \times 10^4\ M^{-1}$ and $\varepsilon = 270\ M^{-1}\,cm^{-1}$.

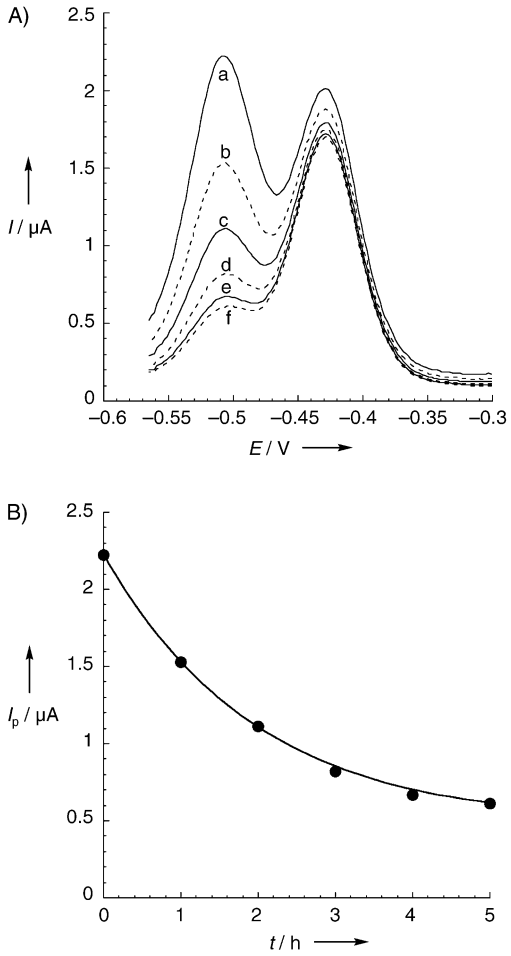

Figure 4. A) Differential pulse voltammograms of the **2**–FAD-functionalized Au electrode upon its reconstitution with apo-GOx, 1 mg mL^{-1}: a) 0 h, b) 1 h, c) 2 h, d) 3 h, e) 4 h, f) 5 h. DPVs were recorded in phosphate buffer (0.1 M, pH 8.0) under Ar, versus SCE . B) Decrease of the FAD peak upon the reconstitution process.

and [**2**] and [**4**] are the concentrations of the materials **2** and **4**, respectively.) Interestingly, despite the structural differences between the diimine moiety in the monolayer configuration and the model compound **4** in solution, and despite the fact that the association constants for the supramolecular complex of the monolayer assembly and the solute molecular units are determined in different solvents (water and acetone, respectively), very similar association constant values were deduced for the two structures.

The small difference between the potentials of FAD ($E° = -0.51$ V at pH 8) and **2** ($E° = -0.43$ V) did not allow the characterization of the redox components by cyclic voltammetry on the modified electrode. Thus, differential pulse voltammograms (DPVs) were recorded to observe the separate electrochemical responses of FAD and the interlocked redox units **2** (Figure 4A, curve a). As the two redox components FAD[11] and **2**[15] show two-electron-transfer processes, the peaks observed in the DPVs directly relate to the amount of surface-confined molecules. The surface coverage of **2** in the modified layer was estimated to be $\approx 0.8 \times 10^{-10}$ mol cm^{-2} and that of the FAD cofactor stopper $\approx 1 \times 10^{-10}$ mol cm^{-2}.[16]

Figure 4A curves b–f, show the time-dependent changes in the DPVs of the rotaxane-functionalized monolayer electrode upon the reconstitution of apo-GOx on the FAD stopper units. The peak corresponding to the FAD units decreases owing to the insulation of the FAD cofactor upon its reconstitution into the protein, whereas the peak for the complexed **2** is almost unaffected. The surface coverage of the reconstituted GOx ($\approx 2 \times 10^{-12}$ mol cm^{-2}) was derived from QCM measurements. The kinetics of reconstitution of the FAD monolayer into the apo-GOx (Figure 4B) is similar to that observed for other apo-GOx reconstitution systems.[17] The blocking of the FAD electrochemical response upon reconstitution with apo-GOx is not surprising and has been previously observed in other related systems.[5,17] In the free rotaxane–FAD monolayer configuration, the observed redox responses of **2** and FAD are due to the flexibility of the molecular spacer that provides short electron-transfer distances for both components. Upon reconstitution, the monolayer is rigidified and the FAD unit is shielded by the protein backbone thus preventing its direct electrical communication with the electrode.

From the redox potentials of the cyclophane **2** and the FAD units, one may conclude that vectorial electron transfer could be mediated by **2** provided that FAD exists in its biocatalytically generated reduced state. Figure 5A shows the cyclic voltammograms of the reconstituted enzyme electrode with the rotaxane-mediator structure in the presence of variable concentrations of glucose. Electrocatalytic anodic currents corresponding to bioelectrocatalyzed oxidation of glucose are observed at around −0.4 V versus SCE. The current increases as the concentration of glucose is elevated (Figure 5B). A control experiment reveals that the reconstitution of apo-GOx on a FAD monolayer that lacks the

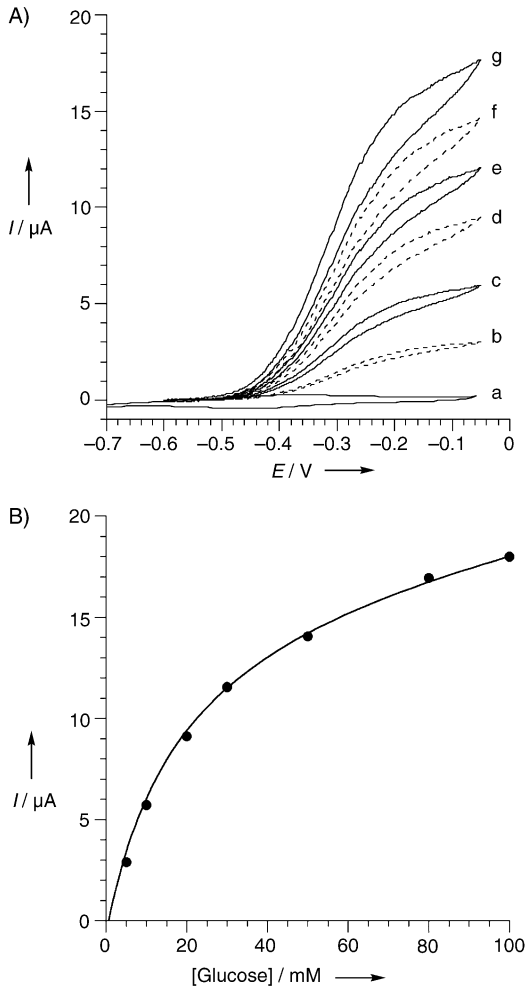

Figure 5. A) Cyclic voltammograms of the GOx-reconstituted electrode at different concentrations of glucose: a) 0 mM, b) 5 mM, c) 10 mM, d) 20 mM, e) 30 mM, f) 50 mM, g) 80 mM. Data were recorded in phosphate buffer (0.1 M, pH 8.0) under Ar. B) Calibration plot for glucose derived from the cyclic voltammograms at −0.1 V.

complex **2** does not yield an electrically contacted enzyme interface, although the biocatalyst is in a structurally active configuration.[18] These results clearly indicate that the monolayer-interlocked **2** acts as an electron-transfer mediator that transports the electrons from the FAD cofactor to the electrode surface. Knowing the surface coverage of the enzyme and the maximum current that is extracted from the system, we calculate an electron-transfer turnover rate of approximately 400 s^{-1}.

The effective electrical contact between the enzyme and the electrode in the rotaxane configuration may be attributed to two factors: 1) The electron-transfer mediator **2** is a two-electron relay, thus complementing the redox features of the FAD cofactor which also involves the transfer of two electrons. 2) The electron-relay **2** loses its electron acceptor properties after accepting the electrons from the FAD cofactor. As a result, the original donor–acceptor complex is perturbed and the reduced relay is free to move on the "molecular wire". This facilitates the transport of electrons to the electrode, resulting in the efficient bioelectrocatalyzed oxidation of glucose.

The dynamic shuttling of the bipyridinium cyclophane **2** on the molecular wire upon its reduction and reoxidation was confirmed by chronoamperometric experiments. The time-dependent current ($I(t)$) generated upon the reduction or the oxidation of a surface-confined redox species is given by Equation (4), in which k_{et} is the rate constant for the electron

$$I(t) = k_{et}\, Q \exp(-k_{et}\, t) \qquad (4)$$

transfer between the redox species and the electrode, and Q is the charge associated with the reduction (or oxidation) of the redox species linked to the electrode.[19]

Previous studies indicate[20] that the interfacial electron-transfer rate constant is controlled by the distance separating the redox unit and the electrode surface. Indeed, several studies[9e,21] have monitored dynamic and structural changes of redox-active components associated with electrodes by following the electron-transfer rate constants at the conductive supports. We have applied the chronoamperometric technique to follow the dynamic shuttling of **2** on the functional molecular wire and to prove that this shuttling occurs upon the mediated bioelectrocatalytic activation of the enzyme. Figure 6A shows the current transient observed upon application of an oxidation potential step on the glucose oxidase-stoppered–rotaxane electrode from −0.45 V to −0.39 V in the absence of glucose. Under these conditions, the cyclophane **2** initially exists in its reduced state and its oxidation proceeds when the potential step is applied. The current transient follows a monoexponential kinetics (Figure 6A, inset) and the derived rate constant and surface coverage of the cyclophane units correspond to $k_{et} = 1100\ s^{-1}$ and 0.8×10^{-10} mol cm^2, respectively. Figure 6B shows the current transient observed upon application of a potential step from −0.39 V to −0.45 V, again in the absence of glucose. Under these conditions, the cyclophane **2** exists in its oxidized state and is reduced to the respective biradical when the potential step is applied. The kinetic analysis (Figure 6B, inset) of the current transient indicates an interfacial electron-transfer rate constant that corresponds to $k_{et} = 80\ s^{-1}$. Thus, reduction of the cyclophane proceeds with a substantially lower electron-transfer rate constant than the oxidation process. This is consistent with the fact that the oxidized cyclophane is localized on the π-donor site by π-donor–acceptor interactions (even though the electrode is negatively charged), and the spatial separation of the redox-active cyclophane **2** from the electrode results in the slow electron-transfer rate. Reduction of the cyclophane unit results in the dissociation of the supramolecular complex on the wire. As the electrode is negatively charged, the positively charged reduced cyclophane is attracted to the electrode and the resulting short distance with respect to the electrode leads to fast electron transfer upon oxidation of the reduced cyclophane.

The position of the cyclophane on the molecular wire upon bioelectrocatalyzed oxidation of glucose by the functionalized enzyme-stoppered–rotaxane assembly was also confirmed by chronoamperometry. Figure 7 shows the current

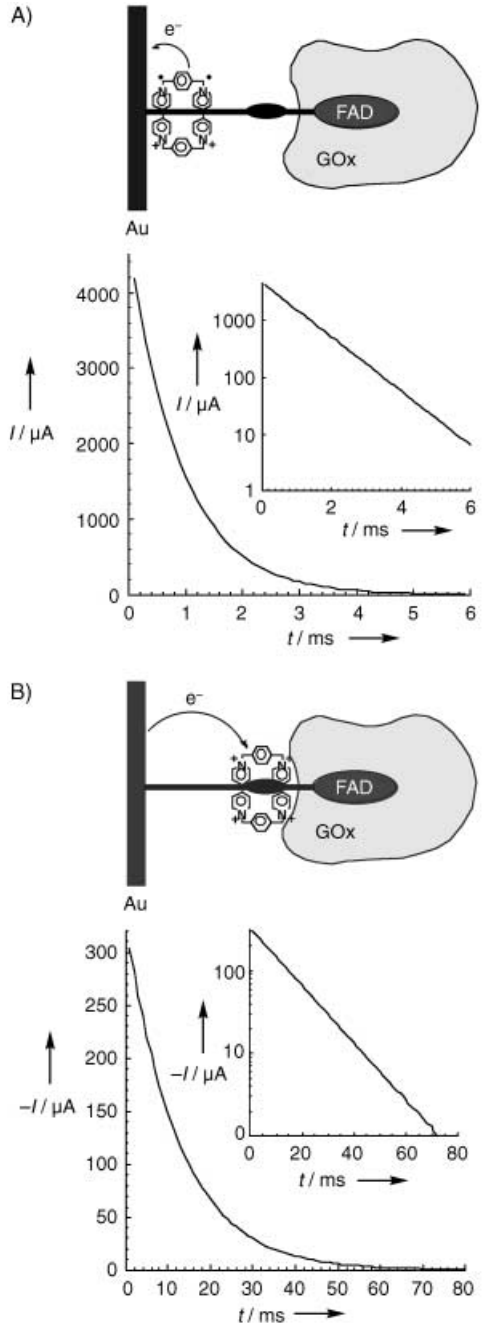

Figure 6. Current transients observed upon application of a potential step; A) from −0.45 to −0.39 V on the enzyme-stoppered–rotaxane electrode (pre-biased at −0.45 V for 10 s). Inset: Kinetic analysis of the current transient curve. B) From −0.39 to −0.45 V on the enzyme-stoppered–rotaxane electrode (pre-biased at −0.39 V for 10 s); Inset: Kinetic analysis of the current transient. All data were recorded in phosphate buffer (0.1 M, pH 8.0) under Ar in the absence of glucose.

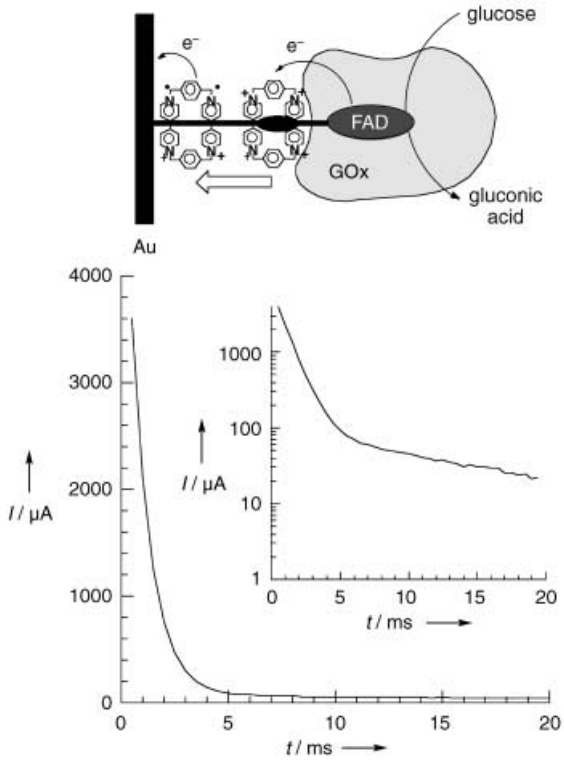

Figure 7. Current transient observed upon the application of a potential step from the open-circuit potential to −0.39 V in the presence of a glucose solution (80 mM) in phosphate buffer (0.1 M, pH 8.0) under Ar. Inset: Kinetic analysis of the experimental current transient curve.

transient upon application of the oxidative step from the open circuit potential to −0.39 V in the presence of glucose (80 mM). This potential step leads to the oxidized form of **2**; the current implies that under the open-circuit conditions the cyclophane exists in its reduced state. The inset in Figure 7 shows the kinetic analysis of the current transient; a fast exponential electron-transfer process is observed (k_{et} = 1100 s^{-1}) followed by a slow nonexponential current tail. The fast electron-transfer rate constant is characteristic of the oxidation of the reduced biradical cyclophane that is in close proximity to the electrode. The slow current transient is attributed to the electrocatalytic anodic current that is developed in the system. These results confirm the functions of the rotaxane as an electron-transfer shuttle in the activation of the enzyme. Under open-circuit conditions, oxidation of glucose leads to reduction of the rotaxane **2** located on the π-donor site and this results in the displacement of the reduced biradical cyclophane to a position that is close to the electrode. The oxidation of the reduced cyclophane reorganizes **2** on the π-donor site leading to the cyclic electrocatalytic activation of the enzyme.

In conclusion, the present study has demonstrated a novel method for the electrical contacting of a redox enzyme by using a rotaxane electron relay interlocked on a molecular wire connecting the enzyme to the electrode. Besides the fundamental interest of the study in establishing a new supramolecular configuration for the bioelectrocatalytic activation of enzymes, the fact that the bioelectrocatalyzed oxidation of glucose by glucose oxidase is activated at a redox potential of around −0.4 V has important practical implications. The nano-structured electrode reveals the lowest possible potential for the oxidation of glucose and thus represents the optimal electrode configuration (anode) for a glucose-based biofuel-cell element. The incorporation and

examination of this electrode in biofuel cells is underway in our laboratory.

Experimental Section

Chemicals: Apo-glucose oxidase (apo-GOx) was prepared by a modification[5b] of a reported method.[22] N^6-(2-Aminoethyl)-flavin adenine dinucleotide (N^6-(2-aminoethyl)-FAD)[23] and cyclobis(paraquat-*p*-phenylene) (**2**)[24] were synthesized and purified as described before. *p*-Dipropyliminobenzene (**4**) was prepared by stirring a mixture of propionic aldehyde (15 mL) and 1,4-diaminobenzene (4.65 g) in dichloromethane (50 mL) overnight at room temperature. The solvent was then evaporated, and the product was recrystallized from ethanol (~80%); ^{1}H NMR (300 MHz; $CDCl_3$): $\delta = 1.2$–1.5 (t, $J = 25$ Hz, 6H), 1.7–1.9 (m, 4H), 6.8–7.1 (m, 4H), 6.1–6.5 ppm (m, 2H). All other chemicals, including pyrroloquinoline quinone (PQQ), 2,2′-dithio-bis(ethaneamine) (cystamine), 4-(2-hydroxyethyl)-piperazine-1-ethanesulfonic acid sodium salt (HEPES), 1-ethyl-3-(3-dimethylaminopropyl)-carbodiimide (EDC), glutaric dialdehyde, β-D-(+)-glucose, and ferrocene monocarboxylic acid, were purchased from Sigma–Aldrich and used as supplied. Ultrapure water (Seralpur Pro 90 CN) was used in all experiments.

Modification of Electrodes: Au electrodes (0.5 mm diameter Au wire, geometrical area ≈0.24 cm^2, roughness factor ≈1.2) were used for modifications. The Au electrodes were cleaned and modified with a self-assembled cysteamine monolayer as described before.[12] The cysteamine monolayer-functionalized electrodes were treated with glutaric dialdehyde (10% v/v) for 20 min. This and all other modification steps were performed in phosphate buffer (0.1M, pH 8.0). After each modification step the electrodes were rinsed with water. The aldehyde-functionalized electrodes were treated with *p*-phenylenediamine (10 mM) for 20 min. The *p*-phenylenediamine-functionalized electrodes were again treated with glutaric dialdehyde (10% v/v) for 20 min to yield diiminobenzene groups on the molecular wire. To analyze the appearance and disappearance of surface amino groups during the modification steps, sample electrodes after each modification step were treated with PQQ (1 mM, in 0.1M HEPES-buffer, pH 7.2) in the presence of EDC (1 mM) for 2 h. The PQQ units covalently attached to the amino groups were assayed by cyclic voltammetry.[12] The electrodes functionalized with the diiminobenzene groups were treated with different bulk concentrations of the rotaxane **2** to generate donor–acceptor complexes under equilibrium. The complex formation was probed by chronocoulometry upon the potential step from −0.35 V to −0.5 V. Surface concentration of the redox complex for each bulk concentration of **2** was derived from the chronocoulometric transients.[13] The electrode containing the surface donor–acceptor complex in equilibrium with **2** (0.3 mM) was further treated with N^6-(2-aminoethyl)-FAD (1 mM) for 20 min to generate a stopper on the molecular string. The resulting **2**–FAD-functionalized electrode was treated with apo-GOx (1 mg mL^{-1}). The process was analyzed by differential pulse voltammetry. After 6 h the reconstitution process was completed and the electrode was rinsed of the excess nonreconstituted apo-GOx. The bioelectrocatalytic oxidation of glucose by the reconstituted GOx-electrode was analyzed by cyclic voltammetry. The real surface area of the Au electrode accessible for the electrochemical reactions was found by the chronocoulometric method by using the Cottrell equation.[25] The measurements performed in the presence of $[Fe(CN)_6]^{3-}$ on a bare Au electrode and the diiminobenzene-functionalized Au electrode show that the electrochemically accessible electrode area is not affected by the formation of the monolayer. All modification steps were repeated on a QCM electrode to perform microgravimetric analyses of the components bound to the surface.

Electrochemical and microgravimetric measurements: A conventional three-electrode cell, consisting of the modified Au working electrode, a glassy carbon auxiliary electrode isolated by a glass frit, and a saturated calomel reference electrode (SCE) connected to the working volume with a Luggin capillary was used for the electrochemical measurements. All potentials are reported with respect to the SCE. Argon bubbling was used to remove oxygen from the solutions in the electrochemical cell, unless otherwise stated. The cell was placed in a grounded Faraday cage. Cyclic voltammetry, differential pulse voltammetry, and chronocoulometry were performed on an electrochemical analyzer composed of a potentiostat/galvanostat (EG&G model 283) connected to a computer (EG&G software no. 270/250). A QCM analyzer (Fluke 164T multifunction counter, 1.3 GHz, TCXO) and quartz crystals (AT-cut, 9 MHz, Seiko) sandwiched between two Au electrodes (area 0.196 cm^2, roughness factor ≈3.2) were employed for the microgravimetric analyses in air and in the liquid phase using a flow-cell. The QCM crystals were calibrated by electropolymerization of aniline in H_2SO_4 (0.1M) and Na_2SO_4 (0.5M) electrolyte solution, followed by coulometric assay of the resulting polyaniline film and relating the crystal frequency changes to the electrochemically derived polymer mass.

Received: December 3, 2003
Revised: March 22, 2004 [Z53455]

Keywords: biosensors · electron transfer · enzymes · molecular devices · monolayers

[1] a) E. Katz, A. N. Shipway, I. Willner in *Encyclopedia of Electrochemistry*, *Vol. 9* (Eds.: G. S. Wilson, A. J. Bard, M. Stratmann), Wiley-VCH, Weinheim, **2002**, chap. 17, pp. 559–626; b) I. Willner, E. Katz, *Angew. Chem.* **2000**, *112*, 1230–1269; *Angew. Chem. Int. Ed.* **2000**, *39*, 1180–1218; c) A. Heller, *Acc. Chem. Res.* **1990**, *23*, 128–134; d) F. A. Armstrong, G. S. Wilson, *Electrochim. Acta* **2000**, *45*, 2623–2645.

[2] a) E. Katz, A. N. Shipway, I. Willner in *Handbook of Fuel Cells—Fundamentals, Technology, Applications*, *Vol. 1*, *Part 4* (Eds.: W. Vielstich, H. Gasteiger, A. Lamm), Wiley, New York, **2003**, chap. 21, pp. 355–381; b) E. Katz, I. Willner, A. B. Kotlyar, *J. Electroanal. Chem.* **1999**, *479*, 64–68; c) E. Katz, I. Willner, *J. Am. Chem. Soc.* **2003**, *125*, 6803–6813; d) N. Mano, F. Mao, A. Heller, *J. Am. Chem. Soc.* **2003**, *125*, 6588–6594.

[3] a) Y. Degani, A. Heller, *J. Phys. Chem.* **1987**, *91*, 1285–1289; b) W. Schuhmann, T. J. Ohara, H.-L. Schmidt, A. Heller, *J. Am. Chem. Soc.* **1991**, *113*, 1394–1397; c) I. Willner, A. Riklin, B. Shoham, D. Rivenzon, E. Katz, *Adv. Mater.* **1993**, *5*, 912–915.

[4] a) A. Heller, *J. Phys. Chem.* **1992**, *96*, 3579–3587; b) H. Bu, S. R. Mikkelsen, A. M. English, *Anal. Chem.* **1995**, *67*, 4071–4076.

[5] a) I. Willner, V. Heleg-Shabtai, R. Blonder, E. Katz, G. Tao, A. F. Bückmann, A. Heller, *J. Am. Chem. Soc.* **1996**, *118*, 10321–10322; b) E. Katz, A. Riklin, V. Heleg-Shabtai, I. Willner, A. F. Bückmann, *Anal. Chim. Acta* **1999**, *385*, 45–58.

[6] Y. Xiao, F. Patolsky, E. Katz, J. F. Hainfeld, I. Willner, *Science* **2003**, *299*, 1877–1881.

[7] F. Patolsky, Y. Weizmann, I. Willner, *Angew. Chem.* **2004**, *116*, 2165–2169; *Angew. Chem. Int. Ed.* **2004**, *43*, 2113–2117.

[8] a) R. A. Bissell, E. Cordova, A. E. Kaifer, J. F. Stoddart, *Nature* **1994**, *369*, 133–137; b) M. C. T. Fyfe, J. F. Stoddart, *Acc. Chem. Res.* **1997**, *30*, 393–401; c) H. R. Tseng, S. A. Vignon, J. F. Stoddart, *Angew. Chem.* **2003**, *115*, 1529–1533; *Angew. Chem. Int. Ed.* **2003**, *42*, 1491–1495; d) S. J. Rowan, J. F. Stoddart, *Polym. Adv. Technol.* **2002**, *13*, 777–787; e) S. J. Rowan, S. J. Cantrill, G. R. L. Cousins, J. K. M. Sanders, J. F. Stoddart, *Angew. Chem.* **2002**, *114*, 1528–1531; *Angew. Chem. Int. Ed.* **2002**, *41*, 898–952.

[9] a) M. Lahav, A. N. Shipway, I. Willner, *J. Chem. Soc. Perkin Trans. 2* **1999**, *9*, 1925–1931; b) A. B. Kharitonov, A. N. Shipway, I. Willner, *Anal. Chem.* **1999**, *71*, 5441–5443; c) I. Willner, V. Pardo-Yissar, E. Katz, K. T. Ranjit, *J. Electroanal. Chem.* **2001**, *497*, 172–177; d) C. P. Collier, E. W. Wong, M. Belohradsky,

F. M. Raymo, J. F. Stoddart, P. J. Kuekes, R. S. Williams, J. R. Heath, *Science* **1999**, *285*, 391 – 394; e) Y. Luo, C. P. Collier, J. O. Jeppesen, K. A. Nielsen, E. Delonno, G. Ho, J. Perkins, H. R. Tseng, T. Yamamoto, J. F. Stoddart, J. R. Heath, *ChemPhysChem* **2002**, *3*, 519 – 525.

[10] a) L. Sheeney-Haj-Ichia, I. Willner, *J. Phys. Chem. B* **2002**, *106*, 13094 – 13097; b) M. Asakawa, P. R. Ashton, V. Balzani, C. L. Brown, A. Credi, O. A. Matthews, S. P. Newton, F. M. Raymo, A. N. Shipway, N. Spencer, A. Quick, J. F. Stoddart, A. J. P. White, D. J. Williams, *Chem. Eur. J.* **1999**, *5*, 860 – 875; c) P. R. Ashton, V. Balzani, O. Kocian, L. Prodi, N. Spencer, J. F. Stoddart, *J. Am. Chem. Soc.* **1998**, *120*, 11190 – 11191.

[11] a) P. J. Elving, J. E. O'Reilly, C. O. Schmakel in *Methods of Biochemical Analysis*, *Vol. 21* (Ed.: D. Click), Interscience, New York, **1973**; b) G. Dryhurst, *Electrochemistry of Biological Molecules*, Academic Press, New York, **1977**.

[12] a) E. Katz, D. D. Schlereth, H.-L. Schmidt, *J. Electroanal. Chem.* **1994**, *367*, 59 – 70; b) E. Katz, D. D. Schlereth, H.-L. Schmidt, A. J. J. Olsthoorn, *J. Electroanal. Chem.* **1994**, *368*, 165 – 171.

[13] a) F. C. Anson, *Anal. Chem.* **1966**, *38*, 54 – 57; b) A. B. Steel, T. M. Herne, M. J. Tarlov, *Anal. Chem.* **1998**, *70*, 4670 – 4677.

[14] D. A. Buttry, M. D. Ward, *Chem. Rev.* **1992**, *92*, 1355 – 1379.

[15] A. R. Bernardo, J. F. Stoddart, A. E. Kaifer, *J. Am. Chem. Soc.* **1992**, *114*, 10624 – 10631.

[16] The surface coverages cannot be directly derived from the DPVs; they were derived from a cyclic voltammogram recorded at pH 9.5 at which the FAD potential is negatively shifted ($\delta E°/\delta pH \approx 30\ mV\ pH^{-1}$ at $pH > 7$) relative to the pH-independent potential of **2,** to provide separate waves for both redox components in the cyclic voltammogram.

[17] M. Zayats, E. Katz, I. Willner, *J. Am. Chem. Soc.* **2002**, *124*, 14724 – 14735.

[18] The GOx-reconstituted electrode, which lacks the interlocked rotaxane-mediator and thus does not show bioelectrocatalytic oxidation of glucose, was activated in the presence of the diffusional electron-transfer mediator, ferrocene monocarboxylic acid (0.5 mM). Therefore, the reconstituted GOx exists on the surface in the biocatalytically active state.

[19] a) R. J. Forster, L. R. Faulkner, *Anal. Chem.* **1995**, *67*, 1232 – 1239; b) R. J. Forster, *Langmuir* **1995**, *11*, 2247 – 2255; c) R. J. Forster, *Anal. Chem.* **1996**, *68*, 3143 – 3150; d) R. J. Forster, *Analyst* **1996**, *121*, 733 – 741.

[20] E. Katz, I. Willner, *Langmuir* **1997**, *13*, 3364 – 3373.

[21] V. Pardo-Yissar, E. Katz, I. Willner, A. B. Kotlyar, C. Sanders, H. Lill, *Faraday Discuss.* **2000**, *116*, 119 – 134.

[22] D. L. Morris, R. T. Buckler, *Methods Enzymol.* **1983**, 92, 413 – 417.

[23] A. F. Bückmann, V. Wray, A. Stocker in *Methods in Enzymology: Vitamins and Coenzymes, Vol. 280, Part 1* (Ed.: B. B. McCormick), Academic Press, Orlando, **1997**, p. 360.

[24] M. Asakawa, W. Dehaen, G. Labbe, S. Menzer, J. Nouwen, F. M. Raymo, J. F. Stoddart, D. J. Williams, *Org. Chem.* **1996**, *61*, 9591 – 9595.

[25] A. J. Bard, L. R. Faulkner, *Electrochemical Methods: Fundamentals and Applications*, Wiley, New York, **1980**.

